Parasitol Res (2009) 104:1061–1077
DOI 10.1007/s00436-008-1289-5

ORIGINAL PAPER

# New malaria parasites of the subgenus *Novyella* in African rainforest birds, with remarks on their high prevalence, classification and diagnostics

**Gediminas Valkiūnas · Tatjana A. Iezhova · Claire Loiseau · Thomas B. Smith · Ravinder N. M. Sehgal**

Received: 9 November 2008 / Accepted: 12 November 2008 / Published online: 24 December 2008


**Abstract** Blood samples from 655 passerine birds were collected in rainforests of Ghana and Cameroon and examined both by microscopy and polymerase chain reaction (PCR)-based techniques. The overall prevalence of *Plasmodium* spp. was 46.6%, as determined by combining the results of both these diagnostic methods. In comparison to PCR-based diagnostics, microscopic examination of blood films was more sensitive in determining simultaneous infection of *Plasmodium* spp., but both detection methods showed similar trends of prevalence of malaria parasites in the same study sites. *Plasmodium* (*Novyella*) *lucens* n. sp., *Plasmodium* (*Novyella*) *multivacuolaris* n. sp. and *Plasmodium* (*Novyella*) *parahexamerium* n. sp. were found in the olive sunbird *Cyanomitra olivacea* (Nectariniidae), yellow-whiskered greenbul *Andropadus latirostris* (Picnonotidae), and white-tailed alethe *Alethe diademata* (Turdidae), respectively. These parasites are described based on the morphology of their blood stages and a segment of the mitochondrial cytochrome *b* (cyt *b*) gene, which can be used for molecular identification and diagnosis of these species. Illustrations of blood stages of new species are given, and phylogenetic analysis identifies DNA lineages closely related to these parasites. Malaria parasites of the subgenus *Novyella* with small erythrocytic meronts clearly predominate in African passerines. It is probable that the development of such meronts is a characteristic feature of evolution of *Plasmodium* spp. in African rainforest birds. Subgeneric taxonomy of avian *Plasmodium* spp. is discussed based on the recent molecular phylogenies of these parasites. It is concluded that a multi-genome phylogeny is needed before revising the current subgeneric classification of *Plasmodium*. We supported a hypothesis by Hellgren, Križanauskienė, Valkiūnas, Bensch (J Parasitol 93:889–896, 2007), according to which, haemosporidian species with a genetic differentiation of over 5% in mitochondrial cyt *b* gene are expected to be morphologically differentiated. This study emphasises the importance of employing both PCR-based and microscopic methods in taxonomic, ecological and evolutionary investigations of avian haemosporidian parasites.

G. Valkiūnas (✉) · T. A. Iezhova
Institute of Ecology, Vilnius University,
Akademijos 2,
Vilnius-21 08412, Lithuania
e-mail: gedvalk@ekoi.lt

C. Loiseau · R. N. M. Sehgal
Department of Biology, San Francisco State University,
1600 Holloway Ave.,
San Francisco, CA 94132, USA

T. B. Smith
Center for Tropical Research, University of California,
Los Angeles, La Kretz Hall,
Los Angeles, CA 90095, USA

## Introduction

Large numbers of blood samples from African rainforest birds were collected in Ghana and Cameroon during an ongoing study on the effects of deforestation on the distribution of blood parasites in African rainforest birds during 2005–2007. Several previously undescribed species of haematozoa were discovered in this material. Three species of haemosporidian parasites belonging to the families Plasmodiidae and Haemoproteidae (the order Haemosporida) were described recently (Valkiūnas et al. 2008c). In this paper, we describe three additional species of *Plasmodium* using data on the morphology of their blood

stages and sequences of the mitochondrial cytochrome *b* (cyt *b*) gene. These parasites were found in the olive sunbird *Cyanomitra olivacea*, the yellow-whiskered greenbul *Andropadus latirostris* and the white-tailed alethe *Alethe diademata*. These vertebrate hosts are widespread in African rainforests (Borrow and Demey 2005) and serve as convenient model organisms in ecological and evolutionary biology studies for vector-borne blood parasite infections in wildlife (Sehgal et al. 2001, 2005).

The aims of this study were (1) to provide detailed morphological descriptions of the new species, (2) to determine mitochondrial cyt *b* gene sequences, which can be used for molecular identification and diagnosis of these parasites, (3) to determine the phylogenetic relationships and genetic distances among the new species and parasites belonging to other subgenera of *Plasmodium*, (4) to discuss the classification of the new species based on the recent molecular phylogenies of avian haemosporidians, (5) to determine which subgenera of malaria parasites are most prevalent in African rainforest birds and (6) to discuss the value of microscopy in determining the prevalence of malaria infection in naturally infected birds.

## Materials and methods

### Collection of blood samples

The samples were collected in Ghana and Cameroon at 27 sites in both rainy and dry seasons during 2005–2007. In all, samples from 449 adult olive sunbirds, 180 adult yellow-whiskered greenbuls and 26 white-tailed alethe were used in this study. The birds were caught with mist nets and banded. Blood samples were collected from the brachial vein and birds were released with none of the individuals being recaptured.

Two or three blood films were prepared from each bird. Blood films were air-dried within 5–10 s after their preparation. In humid environments, we used a battery-operated fan to aid in the drying of the blood films. Slides were fixed in absolute methanol in the field and then stained with Giemsa in the laboratory. Blood films were examined for 10–15 min at low magnification (×400), and then at least 100 fields were studied at high magnification (×1,000). Detailed protocols of fixation, staining and microscopic examination of blood films were described by Valkiūnas et al. (2008b). Intensity of infection was estimated as a percentage by actual counting of the number of parasites per 1,000 red blood cells or per 10,000 red blood cells if infections were light (i.e. <0.1%), as recommended by Godfrey et al. (1987). To ensure absence of simultaneous infections with haemosporidian parasites in the type material of new species, the entire blood films from type series were examined microscopically at low magnification.

Approximately 50 μl of whole blood was drawn from each bird for subsequent molecular analysis. The samples were fixed in lysis buffer (Sehgal et al. 2001); they were held at ambient temperature in the field and later at −20°C in the laboratory.

### Morphological analysis

An Olympus BX61 light microscope equipped with Olympus DP70 digital camera and imaging software AnalySIS FIVE was used to examine slides, prepare illustrations and to take measurements. The morphometric features studied (Table 1) were those defined by Valkiūnas (2005).

Morphology of the parasites was compared with type material of *Plasmodium* (*Novyella*) *hexamerium* from the song sparrow *Melospiza melodia* (accession no. 629, 630) and with type and voucher material of *Plasmodium* (*Novyella*) *vaughani* from its type vertebrate host the American robin *Turdus migratorius* and additional vertebrate host the blackbird *Turdus merula* (accession nos. 635, 639, 654, 655) in the Garnham Collection at the Natural History Museum, London.

Student's *t* test for independent samples was used to determine statistical significance between mean linear parameters. Prevalences were compared by Yates corrected chi-square test. A *P* value of 0.05 or less was considered significant.

### DNA extraction, PCR amplification and sequencing

DNA was extracted from whole blood following a DNeasy kit protocol (Qiagen, Valencia, CA, USA). Success of each DNA extraction was verified with primers that amplify the gene encoding the brain-derived neurotrophic factor (Sehgal and Lovette 2003).

For *Plasmodium* spp. detection, we used a polymerase chain reaction (PCR) method that amplifies a fragment of the cyt *b* region of the mtDNA with primers L15183: 5′-GTG CAA CYG TTA TTA CTA ATT TAT A-3′ and H15730: 5′-CAT CCA ATC CAT AAT AAA GCA T-3′ (Fallon et al. 2003; Szymanski and Lovette 2005). The cycling profile consisted of an initial denaturing at 94°C for 3 min, followed by 35 cycles of 94°C for 50 s, 53°C annealing for 50 s and 72°C extension for 60 s, and then a final extension at 72°C for 5 min. Positive and negative controls were used. The positive controls were from infected birds, as determined by microscopic examination of blood films, and the negative controls were purified water in place of DNA template, or samples that were consistently void of parasites, as confirmed both by microscopic examination and PCR. We also used an additional nested PCR to amplify a fragment of the cyt *b* of new species of *Plasmodium* from infected birds with the primers HAEMF/HAEMR2–HAEMNF/HAEMNR2 following the protocol of Waldenström et al. (2004).

**Table 1** Morphometry of host cells and mature blood stages of new species of malaria parasites from African rainforest birds ($n$=21)

| Features | Measurements (μm)[a] | | |
|---|---|---|---|
| | *Plasmodium multivacuolaris* Lineage pANLA2 | *Plasmodium lucens* Lineage pCYOL2 | *Plasmodium parahexamerium* Lineage pALDI1 |
| Uninfected erythrocyte | | | |
| Length | 10.9–12.0 (11.4±0.3) | 10.2–12.5 (11.5±0.5) | 10.6–12.3 (11.5±0.5) |
| Width | 5.6–7.0 (6.4±0.4) | 5.4–6.5 (6.0±0.3) | 5.8–6.8 (6.3±0.3) |
| Area | 48.1–67.6 (58.5±4.9) | 47.3–64.5 (55.5±3.8) | 47.5–65.5 (58.2±4.6) |
| Uninfected erythrocyte nucleus | | | |
| Length | 4.9–6.1 (5.6±0.3) | 4.4–6.7 (5.3±0.5) | 5.5–6.9 (5.9±0.3) |
| Width | 2.0–3.0 (2.5±0.2) | 1.9–3.9 (2.3±0.4) | 2.3–3.0 (2.7±0.2) |
| Area | 10.7–14.1 (12.2±0.8) | 9.2–13.7 (11.0±1.2) | 12.3–17.0 (14.2±1.2) |
| Macrogametocyte | | | |
| Infected erythrocyte | | | |
| Length | 11.1–13.5 (12.3±0.7) | 11.6–13.9 (12.6±0.6) | 10.9–13.4 (12.1±0.7) |
| Width | 5.9–7.2 (6.6±0.3) | 4.3–6.6 (5.5±0.6) | 5.5–6.8 (6.1±0.3) |
| Area | 56.3–71.7 (63.3±4.9) | 52.6–64.8 (59.0±3.9) | 50.1–69.0 (60.1±4.2) |
| Infected erythrocyte nucleus | | | |
| Length | 5.1–6.4 (5.7±0.3) | 5.0–6.7 (5.9±0.4) | 5.1–6.2 (5.6±0.3) |
| Width | 2.2–3.2 (2.6±0.3) | 1.9–2.8 (2.2±0.2) | 2.1–3.1 (2.4±0.2) |
| Area | 11.3–14.9 (13.3±1.1) | 11.1–14.8 (12.5±1.0) | 9.5–14.1 (12.2±1.1) |
| Gametocyte | | | |
| Length | 10.5–13.4 (12.1±0.6) | 3.3–5.0 (4.3±0.5) | 10.5–14.7 (12.0±1.2) |
| Width | 2.0–3.0 (2.5±0.3) | 1.9–4.2 (3.0±0.6) | 1.4–2.2 (1.8±0.2) |
| Area | 25.4–35.5 (30.2±2.7) | 6.1–12.8 (9.2±1.6) | 17.8–28.8 (23.5±2.9) |
| Gametocyte nucleus | | | |
| Length | 1.6–3.4 (2.6±0.5) | – | – |
| Width | 1.0–2.0 (1.5±0.3) | – | – |
| Area | 1.7–6.3 (3.2±1.1) | 0.7–1.9 (1.3±0.3) | 1.6–3.7 (2.7±0.7) |
| Pigment granules | 7.0–14.0 (10.3±2.1) | 1.0–3.0 (2.1±0.9) | 4.0–10.0 (6.0±1.6) |
| NDR | 0.4–0.9 (0.6±0.1) | 0.6–1.0 (0.9±0.1) | 0.6–1.0 (0.9±0.1) |
| Microgametocyte | | | |
| Infected erythrocyte | | | |
| Length | 11.5–14.0 (12.3±0.7) | 12.5–14.2(13.2±0.6) | 11.1–13.6 (12.5±0.7) |
| Width | 5.4–7.8 (6.6±0.6) | 5.0–6.1 (5.5±0.3) | 5.7–7.2 (6.3±0.4) |
| Area | 49.6–84.0 (64.4±8.1) | 54.9–67.7 (61.1±3.4) | 53.3–73.2 (63.2±6.8) |
| Infected erythrocyte nucleus | | | |
| Length | 5.1–6.4 (5.7±0.5) | 5.1–6.8 (6.2±0.4) | 5.2–6.2 (5.8±0.3) |
| Width | 2.1–3.0 (2.5±0.3) | 1.9–2.5 (2.2±0.2) | 2.0–2.7 (2.3±0.2) |
| Area | 10.1–15.1 (12.9±1.5) | 10.5–15.7 (12.7±1.3) | 11.1–13.4 (12.2±0.7) |
| Gametocyte | | | |
| Length | 10.7–12.8 (11.7±0.6) | 6.1–10.0 (8.3±1.4) | 11.7–14.2 (12.8±0.8) |
| Width | 2.1–2.8 (2.5±0.2) | 1.2–2.1 (1.7±0.2) | 1.6–2.4 (2.0±0.3) |
| Area | 22.7–33.2 (27.6±2.7) | 8.9–17.2 (12.6±2.1) | 19.9–29.0 (24.7±2.7) |
| Gametocyte nucleus | | | |
| Length | 1.8–2.8 (2.5±0.3) | – | 3.0–5.5 (4.1±0.8) |
| Width | 1.2–2.7 (1.8±0.4) | – | 0.5–1.0 (0.8±0.2) |
| Area | 3.3–7.3 (4.8±1.0) | 1.9–3.5 (2.5±0.5) | 1.1–3.5 (2.7±0.6) |
| Pigment granules | 7.0–14.0 (10.5±2.3) | 1.0–5.0 (2.5±1.1) | 5.0–9.0 (6.5±1.3) |
| NDR | 0.5–0.8 (0.7±0.1) | 0.5–0.9 (0.7±0.1) | 0.8–1.0 (0.8±0.1) |
| Meront | | | |
| Length | 3.9–6.3 (4.6±0.6) | 3.5–6.7 (4.3±0.9) | 3.6–5.0 (4.3±0.4) |
| Width | 1.5–3.0 (2.2±0.4) | 1.6–3.2 (2.3±0.5) | 1.8–3.0 (2.3±0.3) |
| Area | 6.2–11.5 (9.3±1.6) | 6.4–10.3 (8.8±1.1) | 6.2–12.2 (8.9±1.3) |
| Area of globule | 0.6–1.4 (1.0±0.2) | – | 0.2–0.5 (0.3±0.1) |
| No. of pigment granules | 1.0–3.0 (1.8±0.8) | 1.0–3.0 (1.6±0.6) | 1.0–3.0 (1.7±0.7) |
| No. of merozoites | 4.0–6.0 (4.5±0.9) | 6.0–12.0 (8.3±1.7) | 6.0–6.0 (6.0±0.0) |

[a] Minimum and maximum values are provided, followed in parentheses by the arithmetic mean and standard deviation
*NDR* nucleus displacement ratio according to Bennett and Campbell (1972)

PCR products were purified using ExoSap following the manufacturer's instructions (USB Corporation, Cleveland, OH, USA). All lineages were identified by sequencing the PCR products [BigDye (R) version 1.1 sequencing kit, Applied Biosystems, Foster City, CA, USA] on an ABI PRISM 3100 (TM) automated sequencer (Applied Biosystems).

We used both PCR methods to compare the lineages of new species with sequences of parasites belonging to the genus *Plasmodium* deposited in GenBank. Sequences obtained with the nested PCR protocol were used for construction of the phylogenetic tree. The GenBank sequences used were carefully selected to correspond to indisputable morphological identifications (see Valkiūnas et al. 2008a, d).

### Phylogenetic analysis

We used 17 mitochondrial cyt *b* sequences of avian *Plasmodium* spp. from our survey and GenBank. The GenBank accession numbers of these sequences are given in Fig. 5. The sequences were aligned using Sequencer 4.8 (GeneCodes, Ann Arbor, MI, USA). All individual sequences were grouped into a consensus that was 468 bp long with one lineage of *Plasmodium falciparum* used as outgroup (Fig. 5).

The phylogenetic tree was constructed using Bayesian phylogenetics as implemented in mrBayes version 3.1 (Ronquist and Huelsenbeck 2003) after finding an appropriate model of sequence evolution using the software mrModeltest (Nylander 2004). A general time-reversible model including invariable sites (GTR+I) was used. The Bayesian phylogeny was obtained using one cold of two hot Monte Carlo Markov chains, which were sampled every 200 generations over 20 million generations; 100,000 trees were generated. Of these trees, 25% were discarded as burn-in material. The remaining 75,000 trees were used to construct a majority consensus tree.

The sequence divergence between the different lineages (Table 2) was calculated with the use of a Jukes–Cantor model of substitution, with all substitution weighted equally, implemented in the program MEGA 3.1 (Kumar et al. 2004).

## Results

### Prevalence and intensity of malaria infections

Species of *Haemoproteus*, *Leucocytozoon*, *Plasmodium*, *Trypanosoma*, *Isospora*, *Hepatozoon* and microfilaria were recorded. Only species of *Plasmodium* were considered during this study. Malaria parasites of the subgenera *Novyella*, *Giovannolaia* and *Haemamoeba* were identified.

The overall prevalence of *Plasmodium* spp. was 305 of 655 (46.6%), as determined by combining methods of microscopic and PCR-based diagnostics. The great majority of recorded *Plasmodium* infections (86%) were very light (<0.01%), often with a few infected erythrocytes seen in the positive blood films. Simultaneous infections of several *Plasmodium* spp. belonging to the same and different subgenera were recorded in 25.4% of all positive samples. The simultaneous infections were particularly common in the olive sunbird (30.4% of all recorded infections); they were uncommon in the yellow-whiskered greenbul (5.3%) and not recorded in the white-tailed alethe.

**Table 2** The sequence divergence (in percentage) between mitochondrial cytochrome *b* lineages of positively identified species of *Plasmodium*

| Species[a] | 1 | 2 | 3 | 4 | 5 | 6 | 7 | 8 | 9 | 10 | 11 | 12 | 13 | 14 | 15 | 16 | 17 |
|---|---|---|---|---|---|---|---|---|---|---|---|---|---|---|---|---|---|
| 1 *P. ashfordi* | 0 | | | | | | | | | | | | | | | | |
| 2 *P. (Novyella)* sp. | 2.4 | 0 | | | | | | | | | | | | | | | |
| 3 *P. juxtanucleare* | 9.6 | 8.8 | 0 | | | | | | | | | | | | | | |
| 4 ***P. multivacuolaris*** | 8.8 | 8.8 | 6.0 | 0 | | | | | | | | | | | | | |
| 5 *P. globularis* | 7.9 | 8.6 | 5.5 | 4.9 | 0 | | | | | | | | | | | | |
| 6 ***P. parahexamerium*** | 8.6 | 8.8 | 6.0 | 5.3 | 4.2 | 0 | | | | | | | | | | | |
| 7 *P. megaglobularis* | 9.1 | 7.9 | 8.4 | 7.9 | 8.6 | 8.6 | 0 | | | | | | | | | | |
| 8 ***P. lucens*** | 8.6 | 8.8 | 7.7 | 8.8 | 8.1 | 7.9 | 5.8 | 0 | | | | | | | | | |
| 9 *P. gallinaceum* | 9.1 | 9.3 | 8.8 | 9.1 | 10.6 | 9.6 | 5.8 | 6.9 | 0 | | | | | | | | |
| 10 *P. circumflexum* | 6.7 | 6.5 | 7.7 | 7.4 | 7.4 | 6.9 | 4.4 | 6.0 | 5.1 | 0 | | | | | | | |
| 11 *P. cathemerium* | 7.2 | 6.9 | 7.2 | 7.4 | 7.2 | 7.9 | 3.3 | 5.3 | 4.6 | 3.3 | 0 | | | | | | |
| 12 *P. relictum* | 7.9 | 8.4 | 8.1 | 8.4 | 7.9 | 7.9 | 3.7 | 5.8 | 6.2 | 4.2 | 3.3 | 0 | | | | | |
| 13 *P. relictum* | 7.7 | 8.1 | 7.9 | 8.1 | 8.1 | 8.1 | 3.5 | 5.5 | 6.0 | 4.4 | 3.1 | 0.2 | 0 | | | | |
| 14 *P. relictum* | 7.2 | 7.7 | 7.4 | 8.1 | 8.1 | 8.1 | 3.9 | 5.3 | 5.5 | 3.9 | 3.1 | 2.4 | 2.2 | 0 | | | |
| 15 *P. relictum* | 7.4 | 7.9 | 7.7 | 8.4 | 8.4 | 8.4 | 4.2 | 5.5 | 5.8 | 4.2 | 3.3 | 2.6 | 2.4 | 0.6 | 0 | | |
| 16 *P. elongatum* | 7.2 | 7.7 | 8.4 | 8.6 | 8.6 | 8.6 | 6.9 | 7.4 | 6.7 | 6.0 | 6.0 | 6.9 | 6.7 | 5.8 | 6.0 | 0 | |
| 17 *P. elongatum* | 7.2 | 7.7 | 8.4 | 8.6 | 8.6 | 8.6 | 6.9 | 7.4 | 6.8 | 6.0 | 6.0 | 6.9 | 6.7 | 5.8 | 6.0 | 0.0 | 0 |

[a] The species are numbered as in Fig. 5 in which GenBank accession numbers of their lineages are given. The sequence divergence was calculated with the use of a Jukes–Cantor model of substitutions. The names of new species are given in bold

Of 305 recorded *Plasmodium* infections, 73.4% belonged to the subgenus *Novyella* and 21.3% and 19% to the subgenera *Haemamoeba* and *Giovannolaia*, respectively, as determined by microscopic examination of blood films. Molecular diagnostics of the great majority of species belonging to these subgenera has not been developed yet. Species of *Novyella* represented 69%, 83% and 100% of all recorded *Plasmodium* infections in the olive sunbird, yellow-whiskered greenbul and white-tailed alethe, respectively. Overall, the prevalence of *Novyella* species was significantly higher than species of *Haemamoeba* ($P<0.001$) and *Giovannolaia* ($P<0.001$). The overall prevalence of *Haemamoeba* and *Giovannolaia* species did not differ significantly ($P=0.550$). Approximately 17% of all recorded *Plasmodium* infections were not identified to the subgeneric level because only single cells of parasites were seen in the blood films, so their detailed comparison with other species was impossible.

We compared the sensitivity of microscopy and PCR-based detection methods in determining the prevalence of *Plasmodium* infection. The overall prevalence of malaria parasites was 44.3% according to microscopic examination of blood films, and it was 31.8% using PCR-based diagnostics; the difference is significant ($P<0.001$). However, both methods showed a similar trend of prevalence of *Plasmodium* infection in our samples, i. e. the prevalence was high using both diagnostic methods. Microscopy did not detect extremely light infections when just a few cells of parasites were present in each blood film. PCR-based diagnostics underestimated the majority of simultaneous infection of parasites belonging to the subgenera *Novyella*, *Giovannolaia* and *Haemamoeba*.

All new species, which are described in this study, belong to the subgenus *Novyella*.

## Description of parasites

### *Plasmodium* (*Novyella*) *multivacuolaris* n. sp. (Fig. 1 and Table 1)

*Type host* Yellow-whiskered greenbul *Andropadus latirostris* (Passeriformes, Picnonotidae).

*DNA sequences* Mitochondrial cyt *b* lineage pANLA2 (468 bp, GenBank accession no. FJ389157).

*Additional hosts* Unknown.

*Type locality* Zoebefame, Cameroon (2°39′31″ N, 13°23′49″ E, 603 m above sea level).

*Prevalence* Overall prevalence in the yellow-whiskered greenbul was eight of 180 (4.4%). In the type locality, the prevalence was six of 48 (12.5%). According to microscopic examination and PCR diagnostics, all recorded infections were single.

*Distribution* This morphospecies and its lineage pANLA2 have been recorded at five study sites both in primary and secondary forests in Cameroon. This parasite has not been found in European migrants subsequent to their arrival from African wintering grounds. It is probable that this lineage is common in the yellow-whiskered greenbul with patchy distribution in the western African rainforests.

*Site of infection* Mature erythrocytes; no other data.

*Type specimens* Hapantotype (accession number 36782 NS, intensity of parasitemia is 0.2%, *Andropadus latirostris*, Zoebefame, Cameroon, collected by G. Valkiūnas, 25 July 2005) is deposited in the Institute of Ecology, Vilnius University, Vilnius, Lithuania. Parahapantotypes are deposited in the Institute of Ecology, Vilnius University, Vilnius, Lithuania (accession no. 36781 NS), in the US National Parasite Collection, Beltsville, USA (USNPC 101408.01, USNPC 101409) and in the Queensland Museum, Queensland, Australia (G465240, G 465243). Light simultaneous infection of *Haemoproteus* sp., *Leucocytozoon* sp., *Hepatozoon* sp. and *Trypanosoma* sp. were present in the type material.

*Etymology* The species name is derived from English word ‘vacuole’. This name reflects the presence of numerous small closely packed vacuoles in mature macrogametocytes of this parasite (see description of macrogametocytes).

*Trophozoites* (Fig. 1a) are seen in mature erythrocytes; they usually are located subpolar or polar to the nuclei of erythrocytes and do not adhere to the nuclei. The smallest trophozoites are variable in shape, usually irregular or slightly ameboid in outline. The ‘ring’ stage is absent. One prominent light blue, non-refractive globule is present in each advanced trophozoite (Fig. 1a); it remains intact in the trophozoites and erythrocytic meronts. Each globule has a clear rim at its periphery (Fig. 1d); such a rim is present around each globule in the type material and thus appears to be a characteristic feature of this species. The parasite nucleus is prominent and locates close to the globule (Fig. 1a). Cytoplasm is usually invisible; vacuoles were not seen. Fully grown trophozoites possess one or two minute brown pigment granules which are usually located close to the globules; due to small size, it is difficult to distinguish the pigment granules even in advanced trophozoites. The influence of trophozoites on the morphology of infected erythrocytes usually is not pronounced.

*Erythrocytic meronts* (Fig. 1b–h) are seen only in mature erythrocytes; the cytoplasm is scanty, stains pale blue and

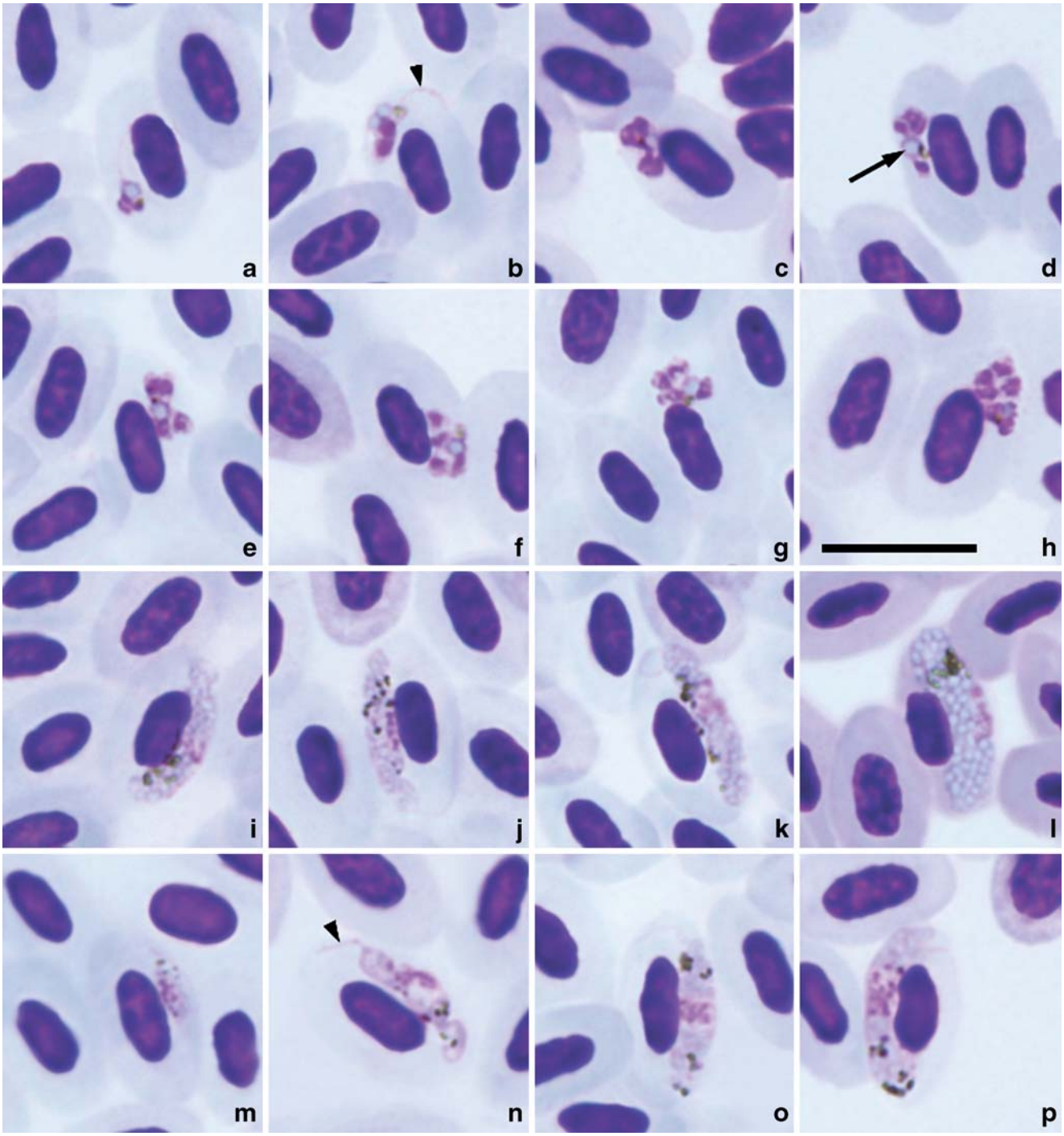


**Fig. 1** *Plasmodium* (*Novyella*) *multivacuolaris* sp. nov. (lineage pANLA2) from the blood of yellow-whiskered greenbul *Andropadus latirostris*: **a** trophozoite; **b**–**h** erythrocytic meronts; **i**–**l** macrogametocytes; **m**–**p** microgametocytes. *Arrow*: bluish non-refractive globule. *Arrowhead*: long thread-like outgrowth. Giemsa-stained thin blood films. Scale bar=10 μm

becomes invisible in fully grown meronts. Growing meronts and advanced trophozoites frequently possess long outgrowths extending far beyond the main body of the parasites (Fig. 1b), which is a characteristic feature of this species. Nuclei are large (Fig. 1c); they decrease in size as the parasite matures (Fig. 1h). Vacuoles are not seen. Meronts usually locate in a subpolar (Fig. 1b–f,h) or polar (Fig. 1g) position to the nuclei of erythrocytes; the advanced parasites frequently adhere to the nuclei (Fig. 1c–h). A light blue, non-refractive globule usually was seen in the more or less central position; it decreases in size and turns into blue colour in maturing meronts

(Fig. 1h). Occasionally, advanced trophozoites with two globules were seen (Fig. 1b). Developing binuclear meronts frequently take a bilobular (bow tie) form with centrally located globules (Fig. 1c). Advanced meronts are irregular in form with irregularly arranged nuclei (Fig. 1f–h). Mature meronts possess four to six, more often six merozoites. Fan-like meronts were not seen. Pigment granules are brown in colour; usually one and two. Occasionally, three minute-sized pigment granules are present in developing meronts; they frequently locate close to globules and are difficult to distinguish. In advanced meronts, pigment granules usually are aggregated into a small mass (Fig. 1g), which usually is located close to the globule. The influence of meronts on the morphology of infected erythrocytes usually is not pronounced, but some parasites can slightly displace nuclei of the erythrocytes (Fig. 1f).

*Macrogametocytes* (Fig. 1i–l) are seen only in mature erythrocytes; the cytoplasm is markedly vacuolated. The vacuoles are roundish in appearance and all are of more or less of similar size. The number of vacuoles increases as the parasite matures and exceeds 30 in each mature gametocyte, with their diameter ranging between 0.3 and 0.6 μm (Fig. 1l). The vacuoles are located homogeneously close to each other in the cytoplasm; they overfill the cytoplasm of mature gametocytes. That gives a distinctive regular multi-spotted appearance to the macrogametocytes (Fig. 1l), which is a unique feature of malaria parasites of birds. Gametocytes are elongated in form and usually slightly irregular in outline from the earliest stages of their development (Fig. 1i,j). Growing gametocytes take a position lateral to the nuclei of infected erythrocytes; they frequently are appressed to the nuclei and can adhere (Fig. 1j) or not adhere (Fig. 1k) to the erythrocyte envelope. Mature gametocytes usually do not fill up the poles of erythrocytes (Fig. 1k,l). Outline of gametocytes varies from irregular (Fig. 1i,j) to even (Fig. 1k,l). The parasite nucleus is of irregular form, usually central in position (Fig. 1l), with its boundaries hardly visible; it possesses prominent granular-like clumps of chromatin. Pigment granules are roundish in form, usually of small (<0.5 μm) size, frequently clumped together into one or several groups, which can be seen anywhere in the gametocytes (Fig. 1k,l). Such clumping makes it difficult to calculate the number of pigment granules. Mature gametocytes displace nuclei of infected erythrocytes laterally, sometimes markedly (Fig. 1l and Table 1).

*Microgametocytes* (Fig. 1m–p). The general configuration and other features are as for macrogametocytes with the usual haemosporidian sexual dimorphic characters; vacuolated appearance of the cytoplasm is much less evident than in macrogametocytes (compare Fig. 1l,p). Long ameboid outgrowths are often present, particularly in growing microgametocytes.

*Remarks P. multivacuolaris* belongs to the subgenus *Novyella*, which unites avian malaria parasites with small erythrocytic meronts and elongated gametocytes (Corradetti et al. 1963, Garnham 1966; Valkiūnas 2005). Twelve species of *Novyella* have been described (Valkiūnas et al. 2008c). None of these species have macrogametocytes with a regular multi-vacuolated appearance (see Fig. 1l), which is a characteristic feature of *P. multivacuolaris*. Cellular composition of these vacuoles remains unknown; investigation of ultrastructure of the gametocytes is needed to answer this question.

*P. multivacuolaris* is most similar to *P. vaughani* and *P. hexamerium*, common parasites of passeriform birds (Bishop and Bennett 1992). Erythrocytic meronts of these species frequently produce six merozoites and have elongate gametocytes. Trophozoites and erythrocytic meronts of *P. hexamerium* do not possess globules (see Fig. 2a), so it can be readily distinguished both from *P. multivacuolaris* and *P. vaughani*.

Trophozoites and erythrocytic meronts of *P. multivacuolaris* and *P. vaughani* possess globules, which is a characteristic feature of development of both these parasites (Manwell 1935; Garnham 1966; Valkiūnas 2005). *P. multivacuolaris* can be readily distinguished from *P. vaughani* (see Fig. 2e–h), primarily due to markedly vacuolated appearance of its macrogametocytes (compare Figs. 1l and 2g) and morphology and the pattern of development of globules. Globules in the erythrocytic meronts of *P. vaughani* are markedly refractive in appearance, with their area ranging between 0.2 and 0.6 $\mu m^2$ (in average 0.4±0.1 $\mu m^2$) in the type material (see Table 1 for size of globules of *P. multivacuolaris*). The difference in area of globules of these two species is significant ($P<0.01$). Additionally, globules change colour and size in erythrocytic meronts of *P. multivacuolaris* as the parasite matures; that is not a case in *P. vaughani*. Furthermore, long ameboid outgrowths are common in growing erythrocytic meronts (Fig. 1b) and microgametocytes (Fig. 1n) of *P. multivacuolaris*, but are absent from the same blood stages of *P. vaughani*.

*Plasmodium* (*Novyella*) *lucens* n. sp. (Fig. 3 and Table 1)

*Type host* Olive sunbird *C. olivacea* (Passeriformes, Nectariniidae).

*DNA sequences* Mitochondrial cyt *b* lineage pCYOL2 (468 bp, GenBank accession no. FJ389156).

*Additional hosts* The lineage pCYOL2 was recorded in one individual of the western bluebill *Spermophaga haematina* in Cameroon.

*Type locality* Nkolowono, Cameroon (4°04′41.3″ N, 11°33′10.9″ E, 617 m above sea level).

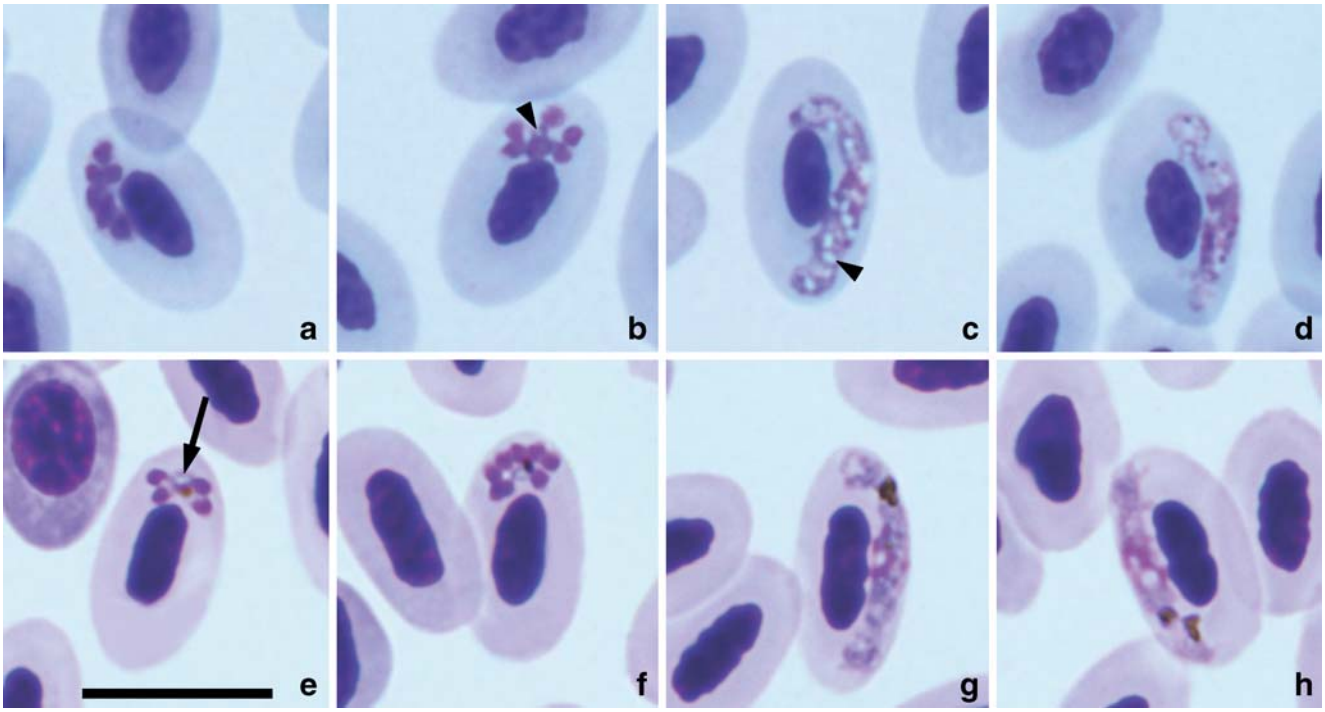


**Fig. 2** *Plasmodium* (*Novyella*) *hexamerium* (**a**–**d**) from the blood of its vertebrate host the song sparrow *Melospiza melodia* and *Plasmodium* (*Novyella*) *vaughani* (**e**–**h**) from its type host the American robin *Turdus migratorius*: **a**, **b**, **e**, **f** erythrocytic meronts; **c**, **g** macrogametocytes; **d**, **h** microgametocytes. *Arrow*: colourless markedly refractive globule. *Arrowheads*: pigment granules which are fading in the type material of *P. hexamerium*, so they look as the colourless spots in **a**–**d**. Giemsa-stained thin blood films. Scale bar=10 μm

*Prevalence* Overall prevalence in the olive sunbird was 47 of 449 (10.5%). In the type locality, the prevalence was six of 21 (28.6%). According to microscopic examination and PCR diagnostics, ten (21.3%) of all recorded infections of *P. lucens* were mixed; among these simultaneous infections, 80% were with other *Plasmodium* spp., 10% with *Haemoproteus* spp. and 10% with both *Plasmodium* spp. and *Haemoproteus* spp. Only samples with single infections were used for the description of *P. lucens*.

*Distribution* This morphospecies and its lineage pCYOL2 have been recorded in three study sites in Ghana and 11 study sites in Cameroon. It is present in birds both in the primary and secondary forests. This parasite has not been found in other African birds, except one individual of the western bluebill. It is absent from European migrants subsequent to their arrival from African wintering grounds. It is probable that *P. lucens* is transmitted throughout the range of the olive sunbird in African rainforests.

*Site of infection* Mature erythrocytes; no other data.

*Type specimens* Hapantotype (accession number 47701 NS, intensity of parasitemia is 0.1%, *C. olivacea*, Nkolowono, Cameroon, collected by T. Dietsch, 17 March 2006) is deposited in the Institute of Ecology, Vilnius University, Vilnius, Lithuania. Parahapantotype (accession number G465245) is deposited in the Queensland Museum, Queensland, Australia. Voucher blood films (accession nos. 41840 NS, 36911 NS and 36912 NS) are deposited in the Institute of Ecology, Vilnius University, Vilnius.

*Etymology* The species name is derived from the Latin word ‘lucens’. This name reflects the presence of one large bright white vacuole in early erythrocytic meronts, particularly in binuclear ones (Fig. 3b). Due to this vacuole, the meronts look like shining bodies, which resemble flashlights; that makes them easy to distinguish in stained blood films.

*Trophozoites* (Fig. 3a) are seen in mature erythrocytes; they can be found anywhere in the host cells but more often are present in the polar or subpolar position to the nuclei of the erythrocytes and do not adhere to the nuclei; variable in shape, sometimes with ameboid outline. The ‘ring’ stage and refractive globules are absent. The parasite nucleus is prominent; the cytoplasm is usually invisible. One prominent vacuole is present in each advanced trophozoite (Fig. 3a). The vacuole remains intact in trophozoites. Fully grown trophozoites possess one or two prominent brown or black pigment granules, which usually are located on the edge of the parasites (Fig. 3a). The influence of trophozoites on the morphology of infected erythrocytes is not pronounced.

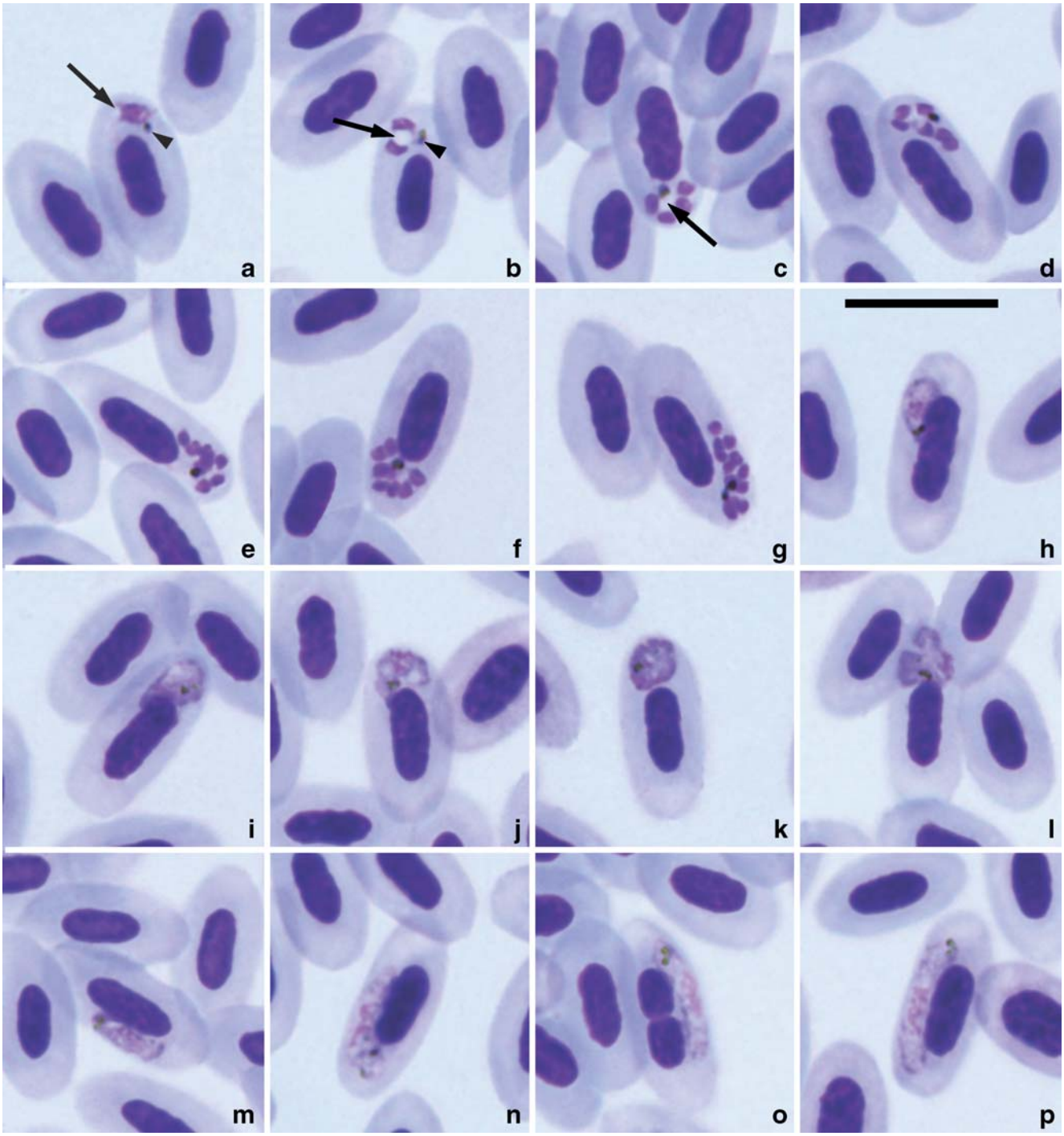


**Fig. 3** *Plasmodium* (*Novyella*) *lucens* sp. nov. (lineage pCYOL2) from the blood of olive sunbird *C. olivacea*: **a** trophozoite; **b**–**g** erythrocytic meronts; **h**–**l** macrogametocytes; **m**–**p** microgametocytes. *Arrows*: white vacuole. *Arrowheads*: pigment granules. Giemsa-stained thin blood films. Scale bar=10 μm

*Erythrocytic meronts* (Fig. 3b–g) are seen only in mature erythrocytes. The cytoplasm is scanty, stains pale blue and becomes very faint even in early meronts (Fig. 3b–d); it is invisible in mature meronts (Fig. 3e–g). Refractive globules are absent. Nuclei decrease in size as the parasite matures. One large bright white vacuole is present in each binuclear and almost each tetranuclear meront (Fig. 3b–c); the vacuole gradually disappears in developing meronts (Fig. 3d,f) and is invisible in mature meronts (Fig. 3g). Binuclear developing meronts are of relatively stable shape; they are of clear 'bow tie' form with a centrally located large vacuole and two prominent nuclei, which are symmetrically arranged on

opposite sides of the vacuole (Fig. 3b). The area of the vacuole ranges between 0.7 and 1.7 (in average 1.2± 0.3) μm$^2$. This binuclear meront is the most easily distinguishable blood stage of this parasite; it is a good diagnostic character of this species. Meronts were seen in polar (Fig. 3b,c,e,f) or subpolar (Fig. 3d,g) positions in infected erythrocytes; they usually do not adhere (Fig. 3b–e, g) or only slightly adhere to the nuclei of erythrocytes (Fig. 3f). Nuclei are arranged as 'bow ties' (Fig. 3b) or fans (Fig. 3c) in binuclear and tetranuclear meronts, respectively. Fully grown meronts usually are irregular in shape with randomly scattered nuclei (Fig. 3d–g). Fan-like mature meronts were not seen. Mature meronts possess six to 12 merozoites. Only two meronts with 12 merozoites were seen (Fig. 3g); the great majority of meronts possess eight merozoites. Pigment granules are brown in colour; they are aggregated into a solid body, which usually is located close to the periphery of each meront (Fig. 3b–e,g). Mature merozoites do not exceed 1 μm in diameter and their cytoplasm is usually invisible (Fig. 3g). The influence of meronts on the morphology of infected erythrocytes usually is not pronounced, but the largest parasites can slightly displace the nuclei of erythrocytes (Fig. 3g).

*Macrogametocytes* (Fig. 3h–l) are seen only in mature erythrocytes; the cytoplasm is homogenous in appearance; a few vacuoles were seen in some gametocytes. Gametocytes are roundish (Fig. 3k), irregular (Fig. 3j), lobulated (Fig. 3l) and comma-like (Fig. 3h,i) in form; elongated gametocytes are absent from the type material. Mature gametocytes take a polar or subpolar position to the nuclei of infected erythrocytes; they are frequently appressed to the nuclei (Fig. 3h–j,l), but parasites not touching the erythrocyte nucleus also are present (Fig. 3k). The parasite nucleus is small, irregular in shape, frequently with a very faint outline and usually off centre in position (Fig. 3j–l). Pigment granules are roundish, of small (<0.5 μm) size, usually clumped together into one group, which usually locates close to the periphery of each gametocyte (Fig. 3h–l). Mature gametocytes slightly displace the nuclei of erythrocytes (Fig. 3l,m). The influence of gametocytes on the morphology of infected erythrocytes usually is not pronounced (Fig. 3h–l).

*Microgametocytes* (Fig. 3m–p) are clearly different from macrogametocytes in form; this is a unique feature for avian malaria parasites. Microgametocytes are elongated in shape from the earliest stages of their development (Fig. 3m); their outline usually is even. Growing microgametocytes take a position lateral to the nuclei of infected erythrocytes; they are appressed to the nuclei (Fig. 3n). Mature microgametocytes are appressed both to the nuclei and envelope of infected erythrocytes; they do not fill up the poles of erythrocytes (Fig. 3o,p). The parasite nucleus is granular in appearance, large, diffuse and central in position (Fig. 3m–p). As usual for haemosporidian parasites, sexual dimorphic characters in morphology of macro- and microgametocytes are well pronounced.

*Remarks* Because of small erythrocytic meronts, the majority of which possess eight merozoites, and the elongated microgametocytes, *P. lucens* belongs to the subgenus *Novyella* (Corradetti et al. 1963; Garnham 1966; Valkiūnas 2005). This malaria parasite can be readily distinguished from other species of *Novyella*, primarily due to (1) the relatively stable shape of its binuclear erythrocytic meronts, which possess large centrally located vacuoles and symmetrically located prominent nuclei (see Fig. 3b) and (2) the clearly different shape of its macro- and microgametocytes (Fig. 3h–p). None of these characters are features of other species of *Novyella* (Valkiūnas 2005; Valkiūnas et al. 2008c)

*Plasmodium* (*Novyella*) *parahexamerium* n. sp. (Fig. 4 and Table 1)

*Type host* White-tailed alethe *A. diademata* (Passeriformes, Turdidae).

*DNA sequences* Mitochondrial cyt *b* lineage pALDI1 (468 bp, GenBank accession no. FJ389155).

*Additional hosts* Unknown.

*Type locality* Nkouak, Cameroon (3°52′1″ N, 13°18′58″ E, 699 m above sea level).

*Prevalence* Overall prevalence in the white-tailed alethe was 18 of 26 (69.2%). In the type locality, the prevalence was two of two (100%). According to microscopic examination and PCR diagnostics, all recorded *Plasmodium* infections were single.

*Distribution P. parahexamerium* and its lineage pALDI1 have been recorded at four study sites in Cameroon and Ghana so far. This parasite is present in birds both in the primary and secondary forests. It has not been found in European migrants subsequent to their arrival from African wintering grounds. It is probable that *P. parahexamerium* is host-restricted and is transmitted in sub-Saharan Africa, where it might be patchy in distribution.

*Site of infection* Mature erythrocytes; no other data.

**Fig. 4** *Plasmodium* (*Novyella*) *parahexamerium* sp. nov. (lineage pALDI1) from the blood of white-tailed alethe *A. diademata*: **a**–**e** trophozoites; **f**–**l** erythrocytic meronts; **m**–**p** macrogametocytes; **q**–**t** microgametocytes. *Arrows*: bluish, refractive globule. Giemsa-stained thin blood films. Scale bar=10 μm

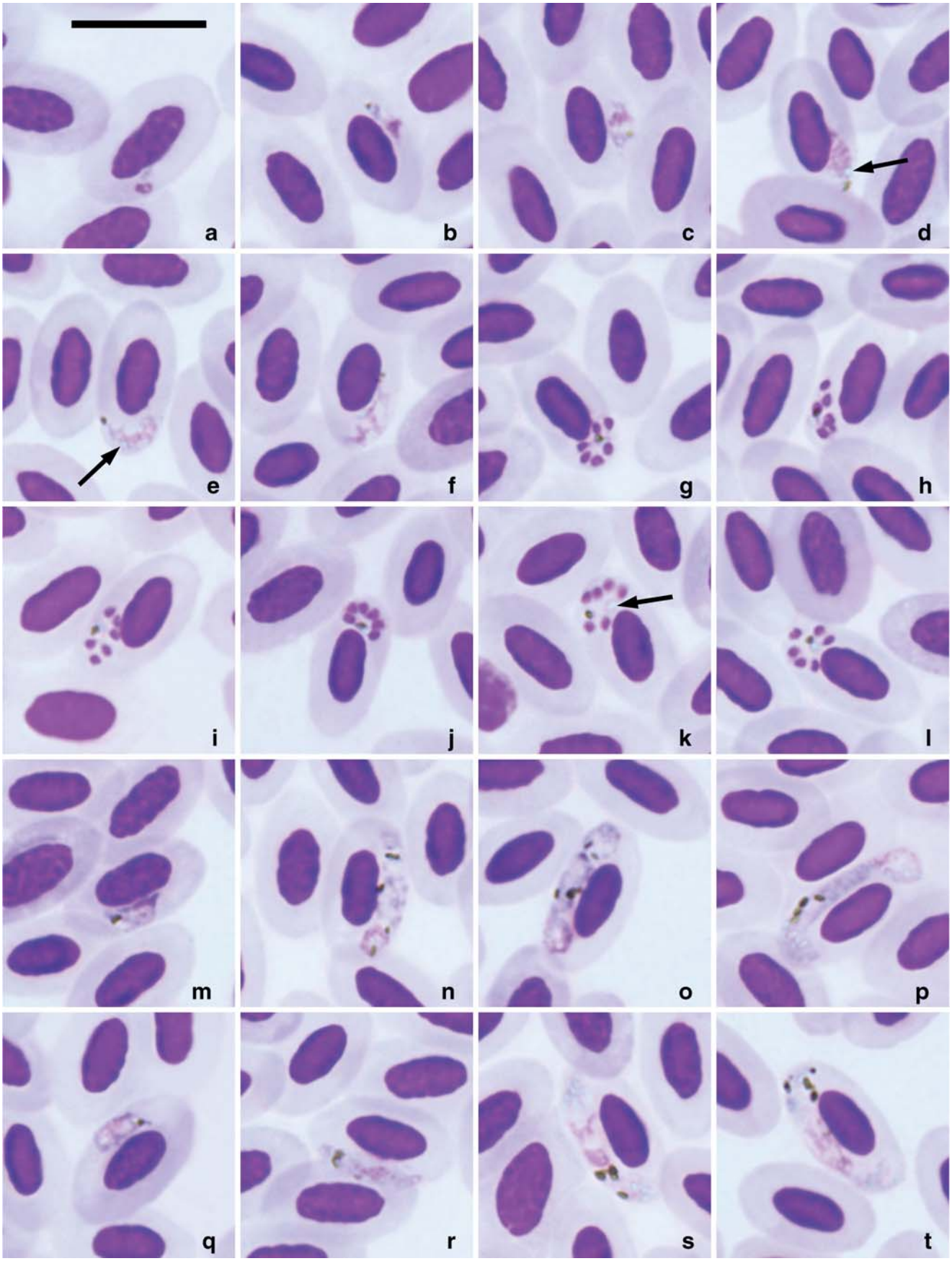
a
b
c
d
e
f
g
h
i
j
k
l
m
n
o
p
q
r
s
t

*Type specimens* Hapantotype (accession number 36124 NS, intensity of parasitemia is 0.1%, *A. diademata*, Nkouak, Cameroon, collected by G. Valkiūnas, 10 July 2005) is deposited in the Institute of Ecology, Vilnius University, Vilnius, Lithuania. Parahapantotypes (accession nos. 36125 NS, 36736 NS, USNPC 101407.01 and G465238) are deposited in the Institute of Ecology, Vilnius University, Vilnius, Lithuania, in the US National Parasite Collection, Beltsville, USA and in the Queensland Museum, Queensland, Australia, respectively. Light simultaneous infections of *Trypanosoma* sp. and microfilaria were present in the type material.

*Etymology* The species name reflects the similarity of erythrocytic meronts of this parasite to *Plasmodium hexamerium* (Huff 1935). Both parasites produce mainly six merozoites in their erythrocytic meronts.

*Trophozoites* (Fig. 2a–e) are seen in mature erythrocytes; they can be found anywhere in the host cells but are more often seen subpolar or polar to the nuclei of erythrocytes. The smallest trophozoites are variable in shape, usually irregular or slightly ameboid in outline. Trophozoites possess prominent nuclei and a prominent cytoplasm (Fig. 4b–e); they usually do not adhere to the nuclei of erythrocytes. The 'ring' stage is absent. One tiny bluish refractive globule appears in each advanced trophozoite (Fig. 4b–e and Table 1); it remains intact in trophozoites, developing and mature erythrocytic meronts. Each fully grown trophozoite possesses a large diffuse nucleus, prominent cytoplasm, one globule and one or two minute brown pigment granules, which are usually located near the edge of the parasite (Fig. 4e). Due to their small size, sometimes it is difficult to distinguish the pigment granules even in advanced trophozoites (Fig. 4d). The influence of trophozoites on the morphology of infected erythrocytes is not pronounced.

*Erythrocytic meronts* (Fig. 4f–l) are only seen in mature erythrocytes. The cytoplasm is prominent and stains pale blue in early meronts (Fig. 4f); it becomes invisible in fully grown meronts (Fig. 4i–l). Nuclei decrease in size as the parasite matures. Vacuoles are not seen. One bluish refractive globule usually locates close to pigment granules (Fig. 4h–j,l), but has also been seen locating more distantly (Fig. 4k). Fully grown meronts usually are roundish or slightly oval in form (Fig. 4g,i,k,l); nuclei are arranged as rosettes (Fig. 4g,k,l), prominent fans (Fig. 4i,j) or irregularly (Fig. 4h) in respect to the order of frequency of their occurrence in the type material. Mature meronts possess strictly six merozoites in all material studied. Between one and three minute brown pigment granules are present in meronts; they are closely clumped in a focus or are aggregated into a prominent mass (Fig. 4i–l), which is easily distinguishable and usually located close to the blue globule. Mature meronts usually are not appressed to the nuclei of infected erythrocytes; they were seen only in polar (Fig. 4g,j–l) or subpolar (Fig. 4h,i) positions relative to the host cell nuclei. Mature merozoites do not exceed 1 μm in diameter; their cytoplasm usually is invisible (Fig. 4l). The influence of meronts on the morphology of infected erythrocytes usually is not pronounced, but nuclei of some infected erythrocytes may be slightly displaced laterally (Fig. 4g,i,k).

*Macrogametocytes* (Fig. 4m–p) are seen only in mature erythrocytes; the cytoplasm is heterogenous (Fig. 4p) or slightly granular (Fig. 4n,o) in appearance. Gametocytes are elongated in form and slightly irregular in outline from the earliest stages of their development (Fig. 4m). Growing gametocytes take a position lateral to the nuclei of infected erythrocytes; they frequently touch the nuclei (Fig. 4n,o). Mature gametocytes frequently do not touch the erythrocyte nuclei but usually are appressed to the erythrocyte envelope (Fig. 4p); they fill up the poles of erythrocytes, enclose the erythrocyte nuclei with their ends but never encircle them completely (Fig. 4p). The parasite nucleus is diffuse and irregular in shape with very faint boundaries; it is terminal in position in each gametocyte and possesses well visible clumps of chromatin (Fig. 4n–p). Pigment granules are oval and rod-like in form, of small (<0.5 μm) and medium (0.5–1.0 μm) size and frequently clumped together; they can be seen anywhere in the gametocytes (Fig. 4p). Small-sized pigment granules were seen only in growing gametocytes (Fig. 4m,n); medium-sized, rod-like pigment granules predominate in mature gametocytes (Fig. 4p). The influence of gametocytes on the morphology of infected erythrocytes usually is not pronounced, but nuclei of some infected erythrocytes may be slightly displaced laterally (Fig. 4o).

*Microgametocytes* (Fig. 4q–t). The general configuration and other features are as for macrogametocytes, with the usual haemosporidian sexual dimorphic characters; granular appearance of cytoplasm is less evident than in macrogametocytes.

*Remarks* Because of the small erythrocytic meronts and the elongated microgametocytes, *P. parahexamerium* belongs to the subgenus *Novyella* (Corradetti et al. 1963; Garnham 1966; Valkiūnas 2005). This malaria parasite can be readily distinguished from other species of *Novyella*, primarily due to (1) strictly six merozoites in its erythrocytic meronts, which possess refractive globules (see Fig. 4l) and (2) the strictly terminal position of nuclei in its mature macrogametocytes. The combination of these characters is not characteristic of other species of *Novyella* (Valkiūnas 2005; Valkiūnas et al. 2008c).

*P. parahexamerium* is most similar to *P. hexamerium*, a common malaria parasite of passeriform birds (Bishop and Bennett 1992). Over 90% of mature erythrocytic meronts of

*P. hexamerium* produce six merozoites (Huff 1935; Valkiūnas 2005); this parasite has elongate gametocytes (see Fig. 2a–d). Trophozoites and erythrocytic meronts of *P. hexamerium* do not possess globules (Fig. 2a,b), so they can be readily distinguished from *P. parahexamerium*. Additionally, nuclei locate centrally in macrogametocytes of *P. hexamerium* (Fig. 2c,d,h), which is not characteristic of *P. parahexamerium* (Fig. 4n–p). Due to these features, the new species can be readily distinguished from *P. hexamerium*.

## Phylogenetic relationships of parasites

The new species belong to different clades in the phylogenetic tree (Fig. 5). The lineage pANLA2 of *P. multivacuolaris* and the lineage pALDI1 of *P. parahexamerium* belong to clade B, with sequence divergence between these two lineages of over 5% (Table 2). The lineage pCYOL2 of *P. lucens* belongs to clade C, with sequence divergence between both *P. parahexamerium* and *P. multivacuolaris* approximately of 8% and 9%, respectively.

Positively identified species of *Novyella* belong to clearly different clades A, B and C in the phylogenetic tree (Fig. 5), with sequence divergence among these species ranging between 4.2% and 9.1% (Table 2). Because these species are paraphyletic in the mitochondrial cyt *b* gene analysis, the subgenus *Novyella* might be invalid. This finding contradicts the traditional taxonomy of avian *Plasmodium* spp. at the subgeneric level.

The lineage pCYOL2 of *P. lucens* belongs to a divergent group of lineages (clade C in Fig. 5) containing nine other lineages of positively identified morphospecies of *Plasmodium*, with a genetic distance between them ranging between 5.3% and 6.9% (Table 2). Parasites of this relatively well-supported clade belong to three subgenera of avian malaria parasites, i.e. *Haemamoeba* (*Plasmodium gallinaceum*, *P. cathemerium*, *P. relictum*), *Giovannolaia* (*P. circumflexum*) and *Novyella* (*P. megaglobularis*, *P. lucens*; Fig. 5). It is important to note that species of *Novyella*, possessing or not possessing globules in their erythrocytic meronts (*P. megaglobularis* and *P. lucens*, respectively), belong to the clade C.

Numerous positively identified species of different subgenera of avian malaria parasites belong to clearly different clades in the phylogenetic tree (Fig. 5, clades A–D), in contradiction to their morphological characteristics. Most striking exceptions are *P.* (*Giovannolaia*) *circumflexum*, *P.* (*Novyella*) *megaglobularis* and *P.* (*Novyella*) *lucens*, which cluster with species of the subgenus *Haemamoeba* (clade C).

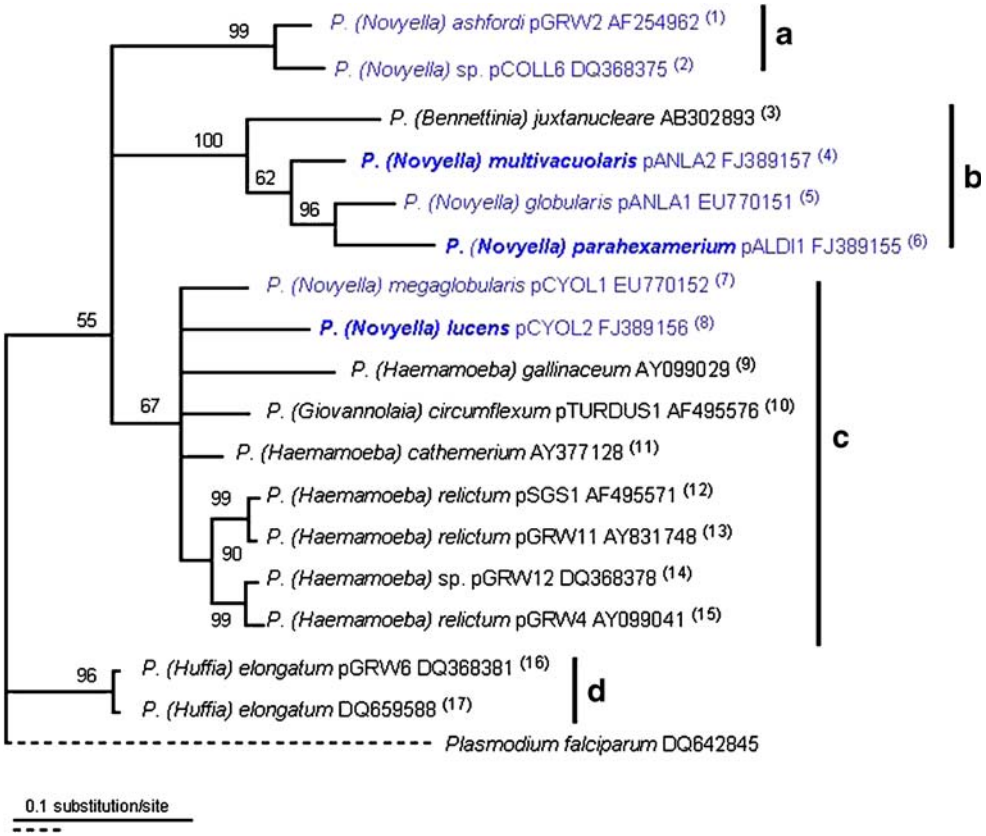


**Fig. 5** Bayesian phylogeny of 17 mitochondrial cytochrome *b* lineages of avian *Plasmodium* spp. and human *P. falciparum* used as an outgroup. Names of the lineages (when available) and GenBank accession numbers of the sequences are given after the parasite species names. The lineages are numbered (*ciphers in parentheses*) as in Table 2. *Vertical bars* indicate species of the subgenera *Novyella* (**a**), *Bennettinia* and *Novyella* (**b**) and *Huffia* (**d**). The *bar C* indicates a group of closely related lineages of *Plasmodium* spp. belonging to the subgenera *Novyella* (*P. megaglobularis*, *P. lucens*), *Giovannolaia* (*P. circumflexum*) and *Haemamoeba* (all other species). The names of new species are given in *bold*. The names of malaria parasites of the subgenus *Novyella* are given in *blue*. The branch lengths are drawn proportionally to the amount of changes (scale bars are shown)

## Discussion

There are numerous molecular studies describing lineages and their prevalences in birds. However, a few of these lineages have been linked with their morphospecies (Sehgal et al. 2006b; Križanauskienė et al. 2006; Martinsen et al. 2007; Palinauskas et al. 2007). Some of the named species in GenBank are misidentifications not only on the species level but even on generic and family levels of taxonomy (Valkiūnas et al. 2008a, d). This is unfortunate because linkage between DNA sequences and identifications based on traditional morphological species can provide important knowledge about basic life history strategies for parasitologists and evolutionary biologists studying phylogenetic relationships, phylogeography and patterns of evolution and distribution of these organisms.

Because of the remarkable genetic and morphological diversity of avian *Plasmodium* spp. (Bensch et al. 2004; Bishop and Bennett 1992; Valkiūnas 2005), it seems probable that the number of new species will increase in the future. Combining morphological and molecular data, six readily distinguishable species of *Novyella* recently were described in African passeriform birds. These are *P. ashfordi*, *P. globularis*, *P. lucens*, *P. megaglobularis*, *P. multivacuolaris* and *P. parahexamerium* (Valkiūnas et al. 2007, 2008c; this study). They are transmitted in Africa, and only *P. ashfordi* is known to infect Palearctic birds at their African wintering areas. *P. ashfordi* has been recorded in several sub-Saharan migrants subsequent to their arrival to Europe from African wintering grounds, but it is not transmitted in Europe (Valkiūnas et al. 2007; Zehtindjiev et al. 2008). The mechanisms that maintain high host and geographical specificity of the sub-Saharan species of *Novyella* remain unclear and may be associated with the particular requirements of these tropical parasites to develop in their vectors, which have been shown to be mosquitoes of the family Culicidae for all studied avian *Plasmodium* spp. (Garnham 1966; Valkiūnas 2005). Investigation into the obstacles for the spread of African *Novyella* species to the northern latitudes might provide new information for understanding the mechanisms of adaptation of avian malaria to new hosts and for better understanding the evolution of these parasites. New species of *Novyella* are convenient model organisms for further investigations into these questions.

According to this study, malaria parasites of the subgenus *Novyella* clearly predominate in African rainforest birds. Reasons for this remain unknown. It is worth noting that species of *Novyella* are the most poorly studied malaria parasites of birds, with markedly fragmented information available about their exoerythrocytic development, mechanisms of relapse and persistence, dynamics of parasitemia, pathogenicity, vectors and development in vectors (Valkiūnas 2005; Zehtindjiev et al. 2008). Experimental studies on the biology of *Novyella* species are lacking in sub-Saharan Africa, which is an obstacle for understanding the ecology, evolutionary biology and pathogenicity of these avian *Plasmodium* spp. Future work in this field should include experimental studies of *Novyella* species, particularly a thorough examination of their vectors.

We used only positively identified morphospecies of avian malaria parasites in phylogenetic analyses (Wiersch et al. 2005; Palinauskas et al. 2007; Valkiūnas et al. 2007, 2008c, d). Sequences of six such species of the subgenus *Novyella* are available in GenBank (Fig. 5). Because these species belong to clearly different clades in the phylogenetic tree, the subgenus *Novyella* might be paraphyletic, in concurrence with Martinsen et al. (2007). These findings show that the current subgeneric classification of avian malaria parasites (Corradetti et al. 1963; Garnham 1966; Valkiūnas 2005) might not reflect the true phylogenetic relationships among avian *Plasmodium* species and may need revision. Because the traditional classification at the subgeneric level reflects morphological diversity of malaria parasites and is useful for their species identification, such a reconstruction should be developed cautiously. It is important to note in this respect that a cladogram from a single molecular sequence (Fig. 5) represents only the phylogeny of that gene, which is not necessary the phylogeny of the species; this is a frequent oversight in apicomplexan parasites (Morrison 2008). For instance, the genus *Plasmodium* was viewed as paraphyletic relative to the genus *Haemoproteus* in a mitochondrial genome phylogeny (Perkins and Schall 2002), but was monophyletic in a recent three-genome phylogeny (Martinsen et al. 2008). To validate the monophyly of *Novyella* species and parasites of other subgenera of *Plasmodium*, additional studies are required that use multi-gene analyses and more lineages from positively identified morphospecies.

It is worth noting that species of *Novyella* are clearly distinguishable due to the presence of globules in their erythrocytic meronts (Garnham 1966; Valkiūnas 2005). This character is distinctive, but has not been formerly been applied in the taxonomy of *Plasmodium*. In some species of *Novyella*, the globules are absent, for instance *P. hexamerium* (Fig. 2), and in some, they are present but are clearly different in their appearance. For instance, erythrocytic meronts of *P. multivacuolaris*, *P. globularis* and *P. megaglobularis* possess large blue, non-refractive globules, which are present in their advanced trophozoites and erythrocytic meronts; such globules have been recorded only in *Novyella* species, which are transmitted in Africa (Valkiūnas et al. 2008c). On the contrary, erythrocytic meronts of *P. vaughani* (Fig. 2) and *P. parahexamerium* (Fig. 4) possess colourless or bluish markedly refractive globules; such globules have been recorded in *Novyella* species all over the world (Iezhova et al. 2005). The biological function and cellular composition

of both types of globules remain unknown. Because species possessing globules (*P. globularis*, *P. multivacuolaris*, *P. parahexamerium*, *P. megaglobularis*) and those that lack them (*P. ashfordi*, *P. lucens*) are not monophyletic in the phylogenetic tree (Fig. 5), it might be that this character developed independently several times during evolution of avian malaria parasites, so might not reflect phylogenetic relationships between *Novyella* species and thus should be applied carefully in the taxonomy of avian *Plasmodium* spp. Again, multi-gene analyses are needed to verify the value of this character in taxonomy of avian malaria parasites.

Hellgren et al. (2007) investigated to what extent morphological species of haemosporidian parasites of the genus *Haemoproteus* are represented by monophyletic groups. They concluded that in most cases, haemosporidian species with a genetic differentiation of over 5% in mitochondrial cyt *b* gene are expected to be morphologically differentiated. Results of our study are in accord with this hypothesis (Table 2). Sequence divergence between new species and all other positively identified species of *Novyella* is over 5% in the mitochondrial cyt *b* gene (Table 2). Interestingly, if the genetic divergence between lineages is >5%, all positively identified species of different subgenera of malaria parasites belong to distinct morphospecies (Table 2). It is probable that different lineages of avian *Haemoproteus* spp., *Plasmodium* spp. and other haemosporidians can be attributed to different morphospecies if the sequence divergence between their mitochondrial cyt *b* lineages is >5%. This criterion provides opportunities to make initial steps in the interpretation of cyt *b* gene phylogenetic trees of avian haemosporidians and in the taxonomy of these parasites on the species level using molecular data. It should be noted, however, that genetic divergence in the cyt *b* gene between some readily distinguishable morphospecies of avian haemosporidian parasites can be as low as 1%, as is the case between *Haemoproteus pallidus* and *Haemoproteus minutus* (Hellgren et al. 2007). Additionally, the sequence divergence is <5% between morphologically distinct *Plasmodium cathemerium* on one hand and *P. megaglobularis*, *P. gallinaceum*, *Plasmodium circumflexum* and *Plasmodium relictum* on the other hand (Table 2). Thus, a molecular criterion of over 5% sequence divergence in cyt *b* gene for the identification of haemosporidian species should be developed and applied carefully, preferably by linking molecular and microscopical data.

The great majority of malaria infections are light in naturally infected birds, often with a few parasite cells present in each blood film (Valkiūnas 2005). Such infections are difficult to identify to the species level using microscopic examination because stages of parasites important for the identification are absent from blood films. That is why numerous publications on haemosporidians provide information mainly about generic or subgeneric identifications of haemosporidians (see Bishop and Bennett 1992; Sehgal et al. 2005; Križanauskienė et al. 2006; Martinsen et al. 2007). Thus, it is essential to develop molecular diagnostics of haemosporidian parasites by adding DNA sequences to the morphological description of species, as is a case in several recent studies (Sehgal et al. 2006a, b; Palinauskas et al. 2007; Valkiūnas et al. 2007, 2008c, d).

It should be noted that simultaneous infections with blood parasites belonging to the same and different genera and subgenera are commonly found in some bird species; they frequently are underestimated by nested PCR (Pérez-Tris and Bensch 2005; Valkiūnas et al. 2006). Thus, cautious consideration is necessary when interpreting sequence data obtained from naturally infected birds, particularly during description of new species. To avoid this problem, we used multiple samples, which were identified as single infections both by PCR-based methods and microscopic examination of entire blood films from the type series.

It is important to note that in previous studies, microscopic examination of blood films was shown to be significantly less sensitive than PCR-based methods in determining prevalence of haemosporidian infections in birds (Richards et al. 2002; Jarvi et al. 2002; Durrant et al. 2006; Fallon and Ricklefs 2008). That raised a question about the value of microscopy in field studies and the reliability of conclusions, which have been based on the microscopy data, in ecology and evolutionary biology of haemosporidian parasites. As concluded by Valkiūnas et al. (2008b), this discrepancy is mainly because (1) blood films of insufficient quality were used or (2) too few microscopic fields were examined, or both, in these comparative studies. For example, in the recent study by Fallon and Ricklefs (2008), maximum 10,000 red blood cells were scanned in each blood films. This is enough to estimate the intensity of infection (Godfrey et al. 1987), but is too small a number of the cells to determine the prevalence of infection, especially in light chronic infections (Garnham 1966; Valkiūnas 2005; Valkiūnas et al. 2008b).

During this study, microscopic detection of malaria parasites was more sensitive in comparison to PCR-based detection methods, but both methods showed the similar trend of prevalence of *Plasmodium* spp. in the same site. The main shortcoming of the currently used PCR-based protocols in detection of haemosporidian infections is the frequent underestimation of simultaneous infections belonging to the same and relative genera of haemosporidians (Valkiūnas et al. 2006); that was also a case during this study.

We conclude that the gold standard of microscopy, which has been a rule in classical studies of haemosporidian parasites since the beginning of the twentieth century (Garnham 1966), is a reliable tool in determining patterns of distribution of blood haemosporidian parasites in naturally infected birds. Minimum requirements for the

microscopic detection of haemosporidian parasites in naturally infected hosts were overviewed by Valkiūnas et al. (2008b); they were followed in this study. We encourage using optical microscopy in studies of blood parasites in parallel to the now widely employed molecular methods. This method of diagnostics is relatively inexpensive and provides valuable information regarding the ways in which how molecular methods can be further improved and most effectively applied, especially in regard to simultaneous infections in the field studies of parasites (Pérez-Tris and Bensch 2005). Importantly, blood films, which are used for microscopic examination, should be of good quality and they should be examined properly by skilled investigators (see Valkiūnas et al. 2008b). In spite of the substantial time investments associated with microscopy, such examination provides opportunities for simultaneous determination and identification of taxonomically different parasites. Presently, different PCR protocols must be used for the detection of blood parasites belonging to different genera; this is expensive and time-consuming.

**Acknowledgements** The authors are grateful to Alan Warren, Natural History Museum, London for providing the type material of *P. vaughani* and *P. hexamerium* and Gillian McIntosh, San Francisco State University for consultations on the Latin language. We would like to thank Anthony Chasar, Tom Dietsch and Augustus Asamoah for help in the field. The present study was supported by the joint NSF-NIH (USA) Ecology of Infectious Diseases Program award EF-0430146, the Lithuanian State Science and Studies Foundation and SYNTHESYS. The investigations described herein comply with the current laws of the USA and Lithuania.

## References

Bennett GF, Campbell AG (1972) Avian Haemoproteidae. III. Description of *Haemoproteus fallisi* n. sp. and a review of the haemoproteids of the family Turdidae. Can J Zool 50:1269–1275

Bensch S, Pérez-Tris J, Waldensrtöm J, Hellgren O (2004) Linkage between nuclear and mitochondrial DNA sequences in avian malaria parasites: multiple cases of cryptic speciation? Evolution 58:1617–1621

Bishop MA, Bennett GF (1992) Host-parasite catalogue of the avian haematozoa: supplement 1; bibliography of the avian blood-inhabiting haematozoa: supplement 2. Mem Univ Newfoundland Occas Pap Biol 15:1–244

Borrow N, Demey R (2005) Birds of Western Africa. Princeton University Press, Princeton

Corradetti A, Garnham PCC, Laird M (1963) New classification of the avian malaria parasites. Parassitologia 5:1–4

Durrant KL, Beadell JS, Ishtiaq F, Graves GR, Olson SL, Gering E, Peirce MA, Milensky CM, Schmidt BK, Gebhard C, Fleischer RC (2006) Avian haematozoa in South America: a comparison of temperate and tropical zones. Ornithol Monogr 60:98–111

Fallon SM, Ricklefs RE (2008) Parasitemia in PCR-detected *Plasmodium* and *Haemoproteus* infections in birds. J Avian Biol 39:514–522

Fallon S, Bermingham E, Ricklefs E (2003) Island and taxon effects in parasitism revisited: avian malaria in the Lesser Antilles. Evolution 57:606–615

Garnham PCC (1966) Malaria parasites and other Haemosporidia. Blackwell Scientific, Oxford

Godfrey RD, Fedynich AM, Pence DB (1987) Quantification of hematozoa in blood smears. J Wildl Dis 23:558–565

Hellgren O, Križanauskienė A, Valkiūnas G, Bensch S (2007) Diversity and phylogeny of mitochondrial cytochrome *b* lineages from six morphospecies of avian *Haemoproteus* (Haemosporida, Haemoproteidae). J Parasitol 93:889–896

Huff CG (1935) *Plasmodium hexamerium*, n. sp. from the blue-bird, inoculable to canaries. Am J Hyg 22:274–277

Iezhova TA, Valkiūnas G, Barlein F (2005) Vertebrate host specificity of two avian malaria parasites of subgenus *Novyella*: *Plasmodium nucleophilum* and *Plasmodium vaughani*. J Parasitol 91:472–474

Jarvi SI, Schultz JJ, Atkinson CT (2002) PCR diagnostics underestimate the prevalence of avian malaria (*Plasmodium relictum*) in experimentally-infected passerines. J Parasitol 88:153–158

Križanauskienė A, Hellgren O, Kosarev V, Sokolov L, Bensch S, Valkiūnas G (2006) Variation in host specificity between species of avian haemosporidian parasites: evidence from parasite morphology and cytochrome *b* gene sequences. J Parasitol 92:1319–1324

Kumar S, Tamura K, Nei M (2004) MEGA3: integrated software for molecular evolutionary genetics analysis and sequence alignment. Brief Bioinform 5:150–163

Manwell RD (1935) *Plasmodium vaughani* (Novy and MacNeal). Am J Hyg 21:180–187

Martinsen ES, Waite JL, Schall JJ (2007) Morphologically defined subgenera of *Plasmodium* from avian hosts: test of monophyly by phylogenetic analysis of two mitochondrial genes. Parasitology 134:483–490

Martinsen ES, Perkins SL, Schall JJ (2008) A three-genome phylogeny of malaria parasites (*Plasmodium* and closely related genera): evolution of life-history traits and host switched. Mol Phylogenet Evol 47:261–273

Morrison DA (2008) Prospects for elucidation the phylogeny of the Apicomplexa. Parasite 15:191–196

Nylander JAA (2004) mrModeltest v2. Program distributed by the author. Evolutionary Biology Centre, Uppsala University. Software available at: <http://www.ebc.uu.se/systzoo/staff/nylander.html>

Palinauskas V, Kosarev V, Shapoval A, Bensch S, Valkiūnas G (2007) Comparison of mitochondrial cytochrome *b* lineages and morphospecies of two avian malaria parasites of the subgenera *Haemamoeba* and *Giovannolaia* (Haemosporida: Plasmodiidae). Zootaxa 1626:39–50

Pérez-Tris J, Bensch S (2005) Diagnosing genetically diverse avian malaria infections using mixed-sequence analysis and TA-cloning. Parasitology 131:1–9

Perkins SL, Schall JJ (2002) A molecular phylogeny of malarial parasites recovered from cytochrome *b* gene sequences. J Parasitol 88:972–978

Richards FA, Sehgal RNM, Jones HI, Smith TB (2002) A comparative analysis of PCR-based detection methods for avian malaria. J Parasitol 88:819–822

Ronquist F, Huelsenbeck JP (2003) MrBayes 3: Bayesian phylogenetic inference under mixed models. Bioinformatics 19:1572–1574

Sehgal RNM, Lovette IJ (2003) Molecular evolution of three avian neurotrophin genes: Implications for proregion functional constraints. J Mol Evol 57:335–342

Sehgal RNM, Jones HI, Smith TB (2001) Host specificity and incidence of *Trypanosoma* in some African rainforest birds: a molecular approach. Mol Ecol 10:2319–2327

Sehgal RNM, Jones HI, Smith TB (2005) Blood parasites of some West African birds. J Vet Med Sci 67:295–301

Sehgal RNM, Hull AC, Anderson NL, Valkiūnas G, Markovets MJ, Kawamura S, Tell LA (2006a) Evidence for cryptic speciation of *Leucocytozoon* spp. (Haemosporida, Leucocytozoidae) in Diurnal Raptors. J Parasitol 92:375–379

Sehgal RNM, Valkiūnas G, Iezhova TA, Smith TB (2006b) Blood parasites of chickens in Uganda and Cameroon with molecular descriptions of *Leucocytozoon schoutedeni* and *Trypanosoma gallinarum*. J Parasitol 92:1336–1343

Szymanski MM, Lovette IJ (2005) High lineage diversity and host sharing of malarial parasites in a local avian assemblage. J Parasitol 91:768–774

Valkiūnas G (2005) Avian malaria parasites and other haemosporidia. CRC, Boca Raton

Valkiūnas G, Bensch S, Iezhova TA, Križanauskienė A, Hellgren O, Bolshakov CV (2006) Nested cytochrome *b* PCR diagnostics underestimate mixed infections of avian blood hemosporidian parasites: microscopy is still essential. J Parasitol 92:418–422

Valkiūnas G, Zehtindjiev P, Hellgren O, Ilieva M, Iezhova TA, Bensch S (2007) Linkage between mitochondrial cytochrome b lineages and morphospecies of two avian malaria parasites, with a description of *Plasmodium* (*Novyella*) *ashfordi* sp. nov. Parasitol Res 100:1311–1322

Valkiūnas G, Atkinson CT, Bensch S, Sehgal RNM, Ricklefs RE (2008a) Parasite misidentifications in GenBank: how to minimise their number? Trends Parasitol 24:247–248

Valkiūnas G, Iezhova TA, Križanauskienė A, Palinauskas V, Sehgal RNM, Bensch S (2008b) A comparative analysis of microscopy and PCR-based detection methods for blood parasites. J Parasitol 94 (in press)

Valkiūnas G, Iezhova TA, Loiseau C, Chasar A, Thomas BS, Sehgal RNM (2008c) New species of haemosporidian parasites (Haemosporida) from African rainforest birds, with remarks on their classification. Parasitol Res 103:1213–1228

Valkiūnas G, Zehtindjiev P, Dimitrov D, Križanauskienė A, Iezhova TA, Bensch S (2008d) Polymerase chain reaction-based identification of *Plasmodium* (*Huffia*) *elongatum*, with remarks on species identity of haemosporidian lineages deposited in GenBank. Parasitol Res 102:1185–1193

Waldenström J, Bensch S, Hasselquist D, Östman Ö (2004) A new nested polymerase chain reaction method very efficient in detecting *Plasmodium* and *Haemoproteus* infections from avian blood. J Parasitol 90:191–194

Wiersch SC, Maier WA, Kampen H (2005) *Plasmodium* (*Haemamoeba*) *cathemerium* gene sequences for phylogenetic analysis of malaria parasites. Parasitol Res 96:90–94

Zehtindjiev P, Ilieva M, Westerdahl H, Hansson B, Valkiūnas G, Bensch S (2008) Dynamics of parasitemia of malaria parasites in a naturally and experimentally infected migratory songbird, the great read warbler *Acrocephalus arundinaceus*. Exp Parasitol 119:99–110